Monitoring the Auroral Oval with GPS and Applications to WAAS

Peter J. Stewart and Richard B. Langley

Geodetic Research Laboratory
Department of Geodesy and Geomatics Engineering
University of New Brunswick

BIOGRAPHIES

Peter Stewart is a Research Assistant at the Department of Geodesy and Geomatics Engineering of the University of New Brunswick, from where he gained an M.Sc.E. Degree in 1997. He also holds a B.Sc. in Topographic Science from the University of Glasgow, Scotland. He is currently researching the effects of the ionosphere on WAAS use in Canadian airspace.

Richard Langley is a professor in the Department of Geodesy and Geomatics Engineering at UNB, where he has been teaching and conducting research since 1981. He has a B.Sc. in applied physics from the University of Waterloo and a Ph.D. in experimental space science from York University, Toronto. Prof. Langley has been active in the development of GPS error models since the early 1980s and is a contributing editor and columnist for GPS World magazine.

ABSTRACT

Mitigation of ionospheric effects in and near the auroral zone is a challenge facing GPS users and service providers in the Canadian north, not the least of which are those promoting augmentations to GPS navigation such as the Wide Area Augmentation System (WAAS). One of the parameters of interest is the location of the auroral oval, the location and extent of which varies with solar and geomagnetic activity. As solar maximum draws ever closer, so periods of enhanced geomagnetic activity will become more frequent, and, consequently, the effect of the auroral ionosphere will become more prevalent at lower latitudes.

Using a number of permanent dual frequency GPS receivers, the location of the auroral oval and its dynamics can be tracked by assuming that the level of ionospheric scintillation will be significantly higher for satellite-receiver paths traversing the oval. Identification of a marked decrease in background ionization will allow estimation of the auroral trough, an area of relatively low ionization found at the equatorward boundary of the oval. Comparison with empirical models of auroral location, such as the Feldstein ovals, provides validation of these results.

We have tested this technique using data from 72 GPS receivers of the International GPS Service and the Continuously Operating Reference System, located north of 45° latitude for two days in May and June 1999 – one when the geomagnetic field was disturbed and one when it was quiet. The results of our initial tests are promising as they show reasonable agreement with both an empirical model and with a satellite-based statistical image.

Enhancement of this technique should allow real time monitoring of the location and extent of the auroral oval, and provide additional information to the WAAS ionospheric message creation process.

INTRODUCTION

The mitigation of ionospheric effects in and near the auroral zone is a challenge facing GPS users and service providers in the Canadian north. One parameter of interest is the location of the auroral oval, the location and extent of which varies with solar and geomagnetic activity [*Hargreaves, 1992*].

Since spatial and temporal variation of ionospheric content in the auroral zone tends to be significantly more rapid than in the surrounding areas, it is suggested that identification of the location of the auroral oval may be achieved by monitoring variations in the measured ionospheric delay.

METHODOLOGY

Data from a network of permanent dual frequency GPS receivers is readily available both from the International GPS Service (IGS) and the National Geodetic Survey Continuously Operating Reference System (CORS). These data provide an ambiguous measure of the ionospheric delay through differencing the L1 and L2 carrier phase observations according to:

$$d_{ion} = \left(\frac{f_2^2}{f_1^2 - f_2^2} \right) \cdot \left(\Phi_1 - \Phi_2 \right)$$

where f_1 and f_2 are the frequencies of the L_1 and L_2 carriers respectively, and Φ_1 and Φ_2 are the carrier phase observations. Since measurements of the incoming carrier phase are biased by an unknown integer number of cycles, a relative rather than absolute estimate of ionospheric delay is obtained. The phase advance measurement is also biased because of differences in the electrical path taken by the L1 and L2 signals both within the satellite and the receiver. These inter-frequency biases (IFBs) can add up to several metres.

This line of sight measurement is mapped to its equivalent vertical value using the simple and widely used geometric mapping function:

$$M(E) = \left[1 - \left(\frac{\cos E}{1 + h/R_e} \right)^2 \right]^{-\frac{1}{2}}$$

where E is the elevation angle measured from receiver to satellite, h is the height of the ionospheric shell upon which the vertical delay is to be mapped and R_e is the Earth's radius.

Figure 1 shows an example of this biased vertical phase advance measured to PRN2 on 18 May 1999 from three stations in Canada for which 30 second sampled data is available via the IGS. It is apparent that the line of sight from PRN2 to Yellowknife passes through a much more active part of the ionosphere than does that from the same satellite to Algonquin. The supposition used in the following analyses is that rapidly changing ionospheric conditions equate to a particular line of sight passing through an active part of the ionosphere, and that this active region is likely to define the auroral zone.

In order to minimize the effects of multipath on the estimates of ionospheric variability, a relatively high elevation angle cutoff of 20 degrees was chosen. This means that all low elevation data for which multipath effects are likely to be most severe are rejected. Note that rejecting low elevation data limits the spatial extent of the data available from each site, and an investigation of the effects of multipath on the estimates of ionospheric variability described here would allow the use of an optimal compromise between multipath rejection and data coverage.

Since we are only interested in the change in ionospheric delay, differencing successive epochs removes the bias (assuming that no cycle slippage has taken place in the intervening period, and that the IFB values are sufficiently stable):

$$\Delta d_{ion} = d_{ion}^{t_k} - d_{ion}^{t_{k-1}}$$

where the superscripts t_k and t_{k-1} refer to the current and previous epoch respectively.

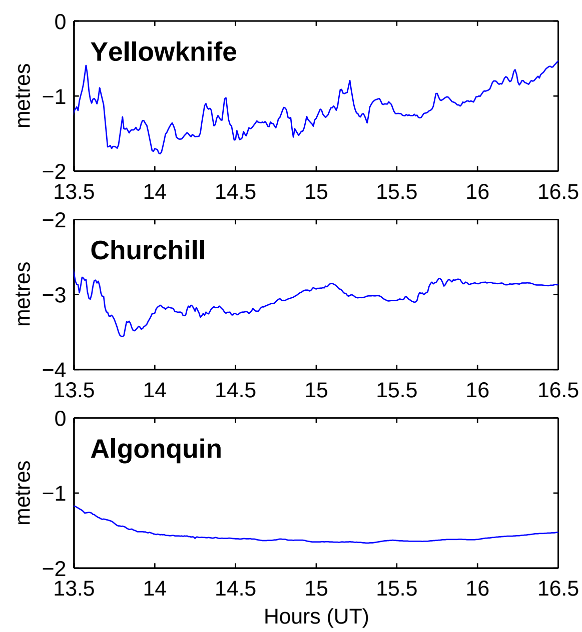

Figure 1. Biased vertical phase advance measured to PRN2 on 18 May 1999 from Yellowknife, NWT, Churchill, MB and Algonquin, ON.

We are therefore able to produce a time series of the variation in ionospheric delay measured along the line of sight to each visible satellite. Computing the standard deviation of this rate of change of ionospheric delay in ten-minute "windows" provides a measure of the local ionospheric variability. Ten-minute data windowing was chosen to allow some averaging of the data without losing too much of the temporal resolution afforded by the 30 second sampling interval.

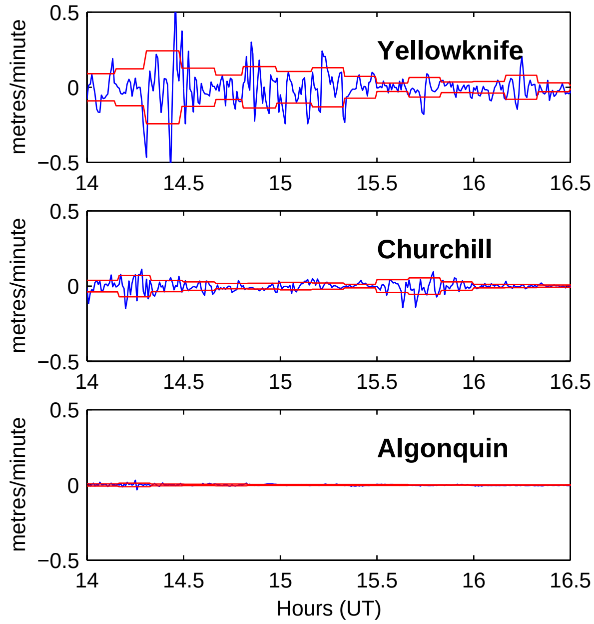

Figure 2. Rate of change of ionospheric delay and its standard deviation evaluated over 10-minute windows.

Figure 2 shows an example of this rate of change measurement for the same three Canadian IGS sites, along with the ten-minute standard deviation. The large standard deviations encountered along the line of sight from PRN2 to Yellowknife reflect much more active ionospheric conditions, and are used as the input parameter for the identification of the location of the auroral oval.

DATA

As was previously mentioned, dual frequency data were collected at 72 stations located throughout the northern latitudes of the Northern Hemisphere. Figure 3 shows the locations of the CORS and IGS sites used in the work described here. A snapshot of the typical data availability is also provided, each triangle indicating the intersection of the line of sight from satellite to receiver with an imaginary shell at an altitude of 350km (the ionospheric pierce point or IPP). This height is chosen to represent the assumed location of structures of the correct scale size to cause fluctuations in the L band GPS signals [*Aarons and Basu, 1994*].

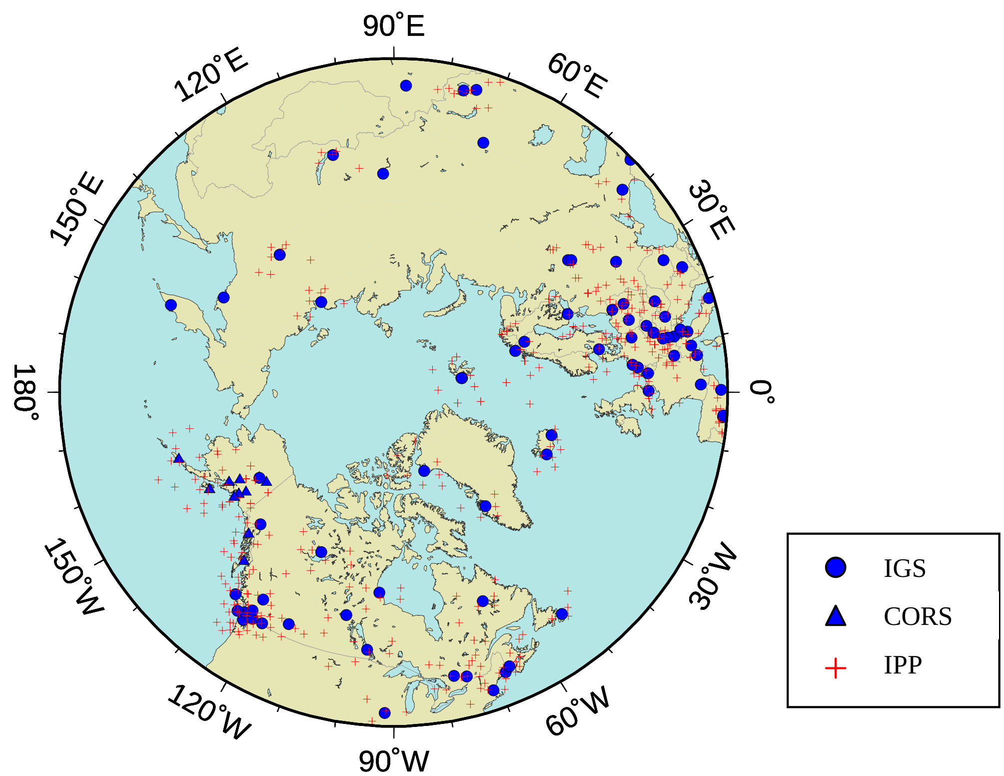

Figure 3. Locations of IGS and CORS stations used. Also plotted to represent typical data distribution are the intersections of the satellite to receiver line of sight with a shell at an altitude of 350km (ionospheric pierce points) at 12 UT on 18 May 1999.

Notice that the stations are far from evenly spaced, and that the distribution of data points (IPPs) is therefore far from optimal. Particularly limiting is the lack of data from the Russian sector. In addition to the relatively few stations in the northern latitudes of Russia (when compared to Western Europe and North America), data availability has also been observed to be far from perfect, and indeed this is reflected in Figure 3 where it can be seen that no IPPs are plotted for two stations in the Russian Far East. Nonetheless, the IGS network of stations provides reasonable coverage, and good results should be expected.

Using the Generic Mapping Tools (GMT) [*Wessel*, *1999*], maps of a surface fit to the ten minute standard deviation associated with each observed IPP were produced. GMT allows the user to input randomly spaced *xyz* triplets of data and form a grid of *z* (*x*,*y*) nodes to which the surface is fit by solving:

$$(1 - T) * L (L (z)) + T * L (z) = 0$$

where T is a tension factor between 0 and 1 (0.25 used here), and L indicates the Laplacian operator. A surface fit to these data points provides an idea of the spatial extent of areas of increased ionospheric activity, and hopefully an indication of the location of the auroral oval.

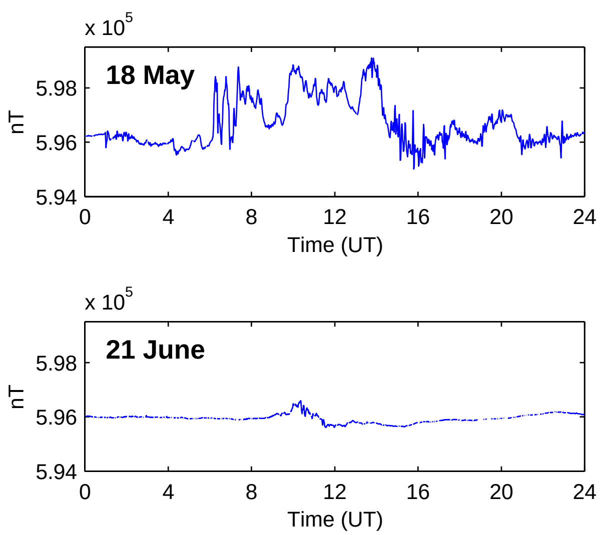

Figure 4. 1 minute mean of the variation of the geomagnetic field measured at Yellowknife, NWT on 18 May and 21 June 1999.

Two days of data in particular were chosen to represent active and quiescent geomagnetic conditions respectively. Figure 4 shows the geomagnetic field variations measured at Yellowknife, NWT on 18 May and 21 June 1999 [*Intermagnet*, *1999*].

Immediately obvious is the order of magnitude difference between the variations on the two days. Since fluctuations in the local geomagnetic field occur as a result of enhanced electric currents flowing in the auroral ionization [*Hargreaves*, *1992*], heightened geomagnetic variability can be seen as a reliable indicator of increased auroral activity. Thus, 18 May has been considered an active day for the purposes of this study and 21 June as a relatively quiet period. It would therefore be expected that the surface interpolated from the standard deviation values described above would reflect these differences.

RESULTS

Figures 5 and 6 below show a series of interpolated surfaces for 18 May and 21 June 1999, with the locations of the data points used to interpolate the surface shown for reference. Also plotted are the poleward and equatorward boundaries of the auroral oval as defined by the algorithm of *Holzworth and Meng* (1975). This mathematical representation of the location of the auroral oval is based on photographs from the Defense Meteorological Satellite Program and the ovals defined by *Feldstein and Starkov* (1967).

Upon inspection of the interpolated surfaces, it is clear that at least some level of correlation exists between the GPS derived data and the *Holzworth and Meng* model, with the diurnal variation of the location of the auroral oval being reflected in the standard deviation of the rate of change of ionospheric delay.

Further comparison is provided by images created by the NOAA Space Environment Center from satellite observations of the power flux in the Earth's atmosphere. The Total Energy Detector, and instrument flown routinely on the NOAA series of polar orbiting satellites, is designed to monitor the power flux carried into the Earth's atmosphere by precipitating auroral charged particles in the energy range from 300 to 20 000 electron volts. More than 100 000 passes have been used to create a number of statistical images of the auroral power flux. The image associated with a particular satellite pass is then chosen from amongst these scenarios based on the observed power flux [*NOAA*, *1999*]. Figure 7 below shows such an image created for approximately the same time represented by the final frame of Figure 5 above.

SUMMARY AND CONCLUSIONS

Large spatial and temporal gradients in the auroral ionosphere can have an effect on GPS and the Wide Area Augmentation System (WAAS) in two ways. Firstly, any ionospheric delay grid model is unlikely to have high enough spatial resolution to adequately represent an active auroral zone. Secondly, rapid variations in the amplitude and phase of the incoming signal (scintillations) can be severe enough to cause losses of lock of the L2 signal. It is therefore important to understand the spatial extent of areas that are likely to have an effect on GPS and WAAS users at northern latitudes.

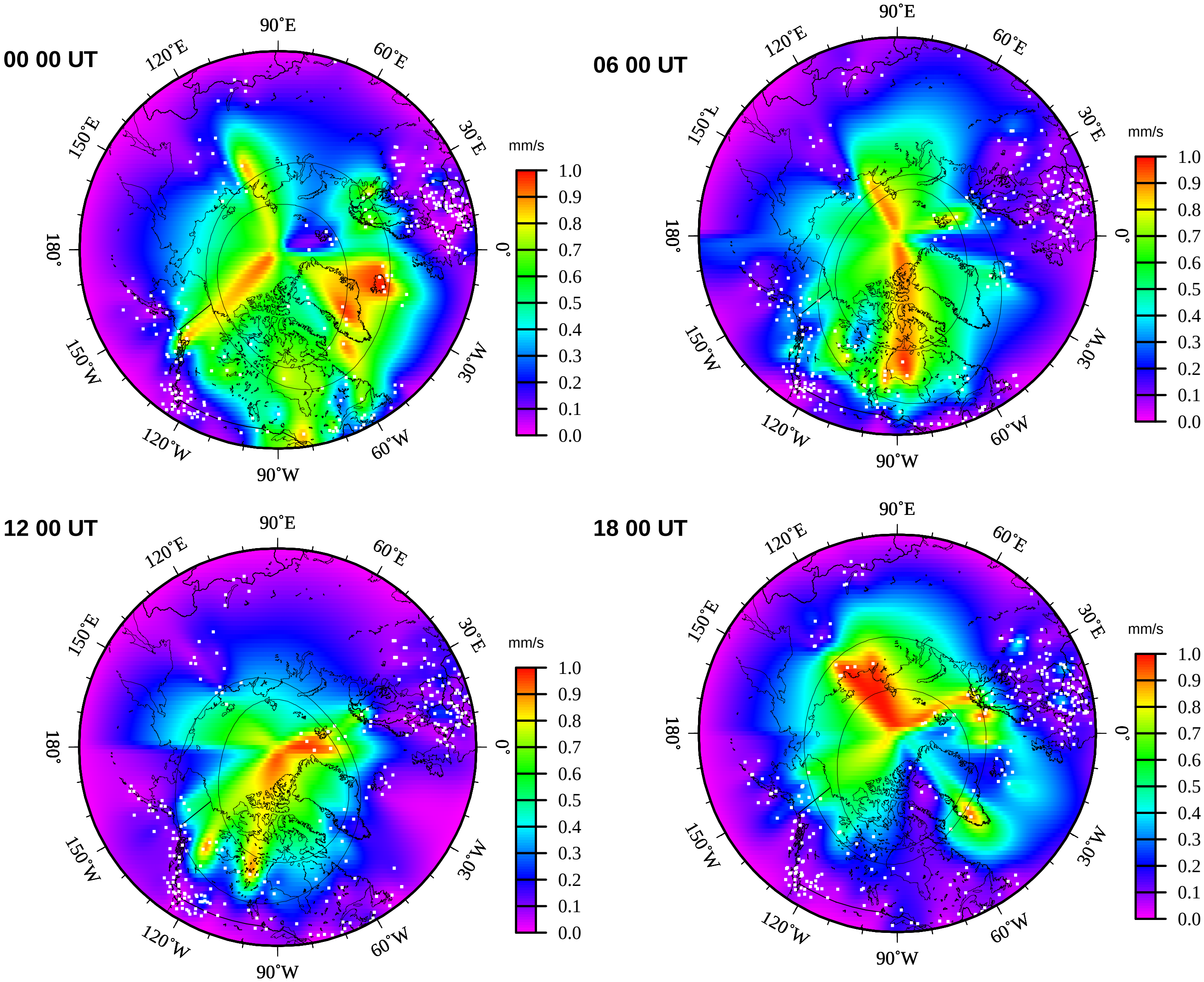

Figure 5. Surface interpolated to the standard deviation parameter described above for various times on 18 May 1999. Also plotted is the location of the *Holzworth and Meng* mathematical model of the auroral oval for each epoch.

Using GPS to monitor the aurora has the advantage of direct sampling of the very effect in which we are interested. Maps such as those shown in Figures 5 and 6 could be used to show the areas over which degradation of performance or signal loss can be expected for various levels of auroral activity.

Our initial study of the possibility of using GPS to track the location of the auroral oval has shown, for the small data set chosen, reasonable agreement with both a mathematical representation [*Holzworth and Meng, 1975*] and a statistical image of the oval.

Limitations of the technique exist because of a lack of data in certain areas of the area in which we are interested, specifically poleward of the auroral oval, and in the northern latitudes of Russia. The general lack of data necessitates a larger than desired reliance on the interpolation scheme, and leads to unwanted artifacts in the surface images produced. Possible improvements of the technique described here include the inclusion of additional data as and when it becomes available, and the application of a Kalman filter to take advantage of the sampling of the temporal correlation of auroral features as they migrate around the region.

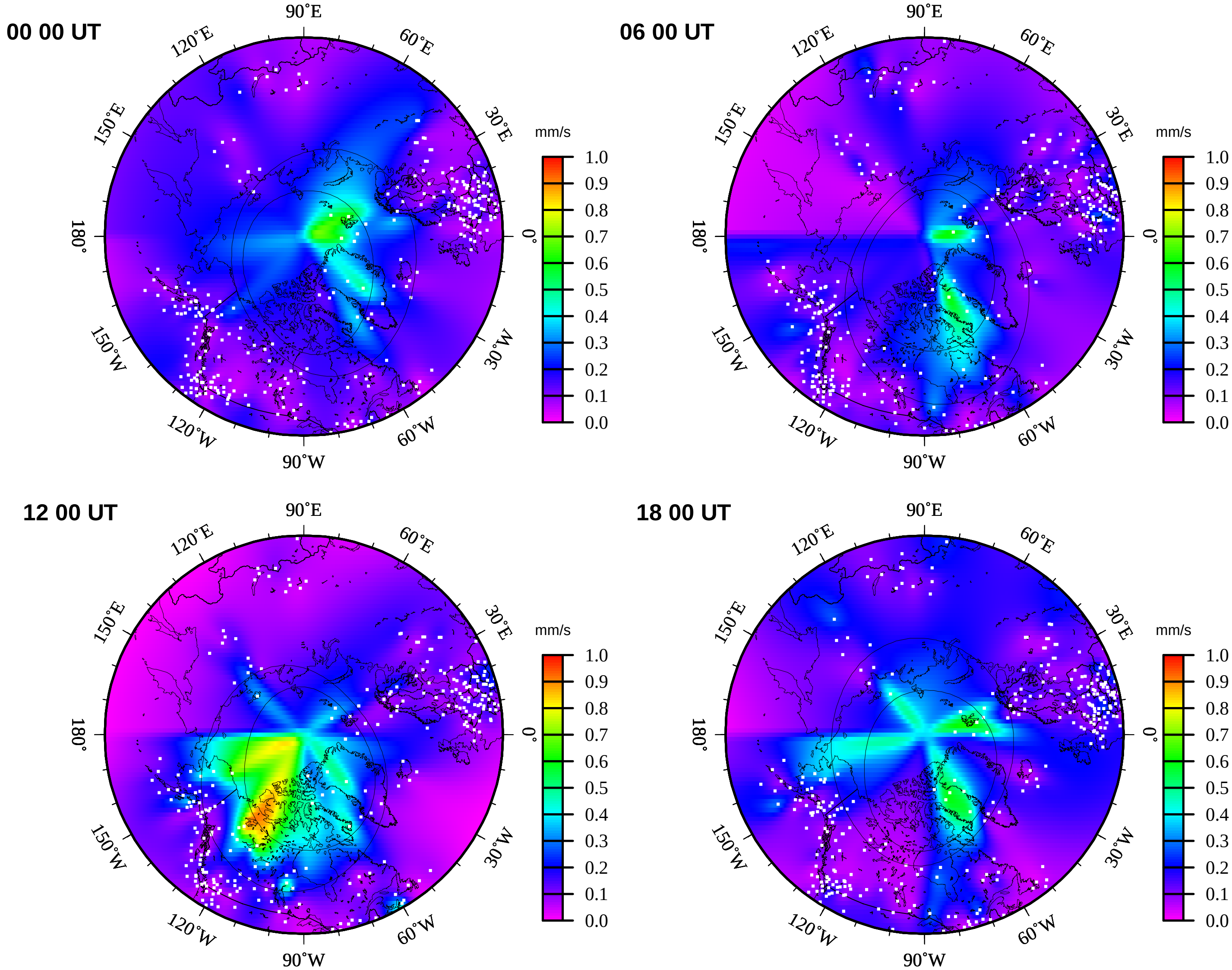

Figure 6. Surface interpolated to the standard deviation parameter described above for various times on 21 June 1999. Also plotted is the location of the *Holzworth and Meng* mathematical model of the auroral oval for each epoch.

A vast data set of dual frequency GPS observations now exists from IGS, CORS and other networks. The National Satellite Test Bed (NSTB), set up by the FAA Tech Center to investigate the feasibility of various WAAS concepts, records 1 Hz data at various sites around the United States and Canada. The data from this network could easily be used to improve the spatial resolution in the Alaskan sector already afforded by the CORS and IGS receivers. Since the processing required to create the maps shown here was relatively simple, production of a time series of auroral activity of sufficient magnitude to affect GPS and WAAS users on an operational level would seem an attainable goal.

The addition of GLONASS data to the monitoring of the auroral oval is likely to increase both the spatial resolution and geographical coverage. The 63-degree orbital inclination of the GLONASS satellites provide better coverage at northern latitudes than does the GPS constellation. The recent International GLONASS Experiment (IGEX) initiative [*ION, 1999*] has provided a source of dual frequency GLONASS data from a few sites in Western Europe, Russia and North America.

ACKNOWLEDGEMENTS

The authors would like to thank Sue Greer of the NOAA Space Environment Center who provided the auroral power flux images used in the work described here. We also thank John Klobuchar for helpful discussions on auroral ionospheric processes.

Funding for our research is provided by Nav Canada's SatNav Program Office.

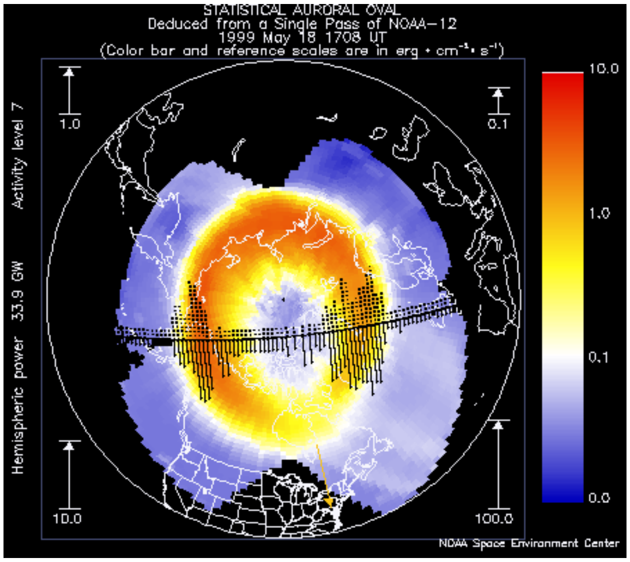

Figure 7. Statistical pattern of auroral power flux based on data from the Total Energy Detector (TED) on board the NOAA-14 satellite. Image provided courtesy of the U.S. Department of Commerce, NOAA, Space Environment Center.

REFERENCES

Aarons, J. and S. Basu (1994). "Ionospheric Amplitude and Phase Fluctuations at the GPS Frequencies", in *Proceedings of ION-GPS-94*, Salt Lake City, UT, 20 – 23 September, 1994, pp. 1569-1578.

Feldstein, Y.I. and G.V. Starkov (1967). "Dynamics of Auroral Belt and Polar Geomagnetic Disturbances." *Planetary and Space Science*, Vol. 15, pp. 209-229.

Hargreaves, J.K. (1992). *The Solar-Terrestrial Environment*, Cambridge Atmospheric and Space Science Series No. 5, Cambridge University Press, Cambridge.

Holzworth, R.H. and C.-I. Meng (1975). "Mathematical Representation of the Auroral Oval", *Geophysical Research Letters*, Vol. 2, No. 9, pp. 377-380.

Intermagnet, (1999). *Geomagnetic Information Nodes Digital Data*. Available: http://www.intermagnet.org/english/gins_e.html#Access. [June 20 1999].

ION (1999). *International GLONASS Experiment [IGEX-98]*. Available http://www.nima.mil/GandG/ion/index.htm [June 26 1999].

NOAA (1999). *Auroral Activity Extrapolated from NOAA/POES*. Available http://www.sel.noaa.gov/pmap/ [June 26 1999].

Wessel, P. (1999). *GMT – The Generic Mapping Tools*. Available: http:// imina.soest.hawaii.edu/gmt/ [June 26 1999].